Proceedings of the 21st International Conference on Global Research and Education (Inter-Academia 2024)

Modelling of Journal Bearings for Predictive Maintenance

J. Nowak[a,b,*] and P. Wnuk[c]

[a] *Faculty of Mathematics, Section Data Science, University of Oslo, Oslo, Norway*
[b] *ABB Business Services, Marine Digital Services, Poland*
[c] *Faculty of Mechatronics, Institute of Automatic Control and Robotics, Warsaw University of Technology, św. A. Boboli 8, 02-525 Warsaw, Poland*

Doi: 10.12693/APhysPolA.146.503 *e-mail: jarek.nowak@gmail.com

Large medium voltage machines such as motors and generators, running with a low speed of less than 1000 rpm, are typically designed with the use of sleeve (or journal) bearings. These machines play a critical role in industrial processes. Sleeve bearings are simple in construction yet designed to operate for many years without any maintenance. Since these are critical components of rotating machines, knowledge about their condition is fundamental. Typical and well-proven methods for condition monitoring of journal bearings are based on measurement of the shaft movement within lubrication oil or monitoring the condition of lubrication oil itself. Both techniques require the installation of special additional sensors that are typically very costly and not necessarily feasible for the systems already in operation. Instead, this article proposes to use existing large data sets of performance-related measurements from rotating machines equipped with sleeve bearings and model them in order to detect anomalies, preferably originating from potential bearing faults. The aim of modelling is to predict bearing temperature as it impacts physically and predictably lubrication oil viscosity and thus lubrication quality. Models derived from both linear and non-linear approximations are to be benchmarked. Since at this stage of analysis, the training process is unsupervised (due to lack of labels for confirmed bearing fault), recommendations given in the article are fundaments for a follow-up work aiming at enriching the data with simulated or field-confirmed bearing defects or suspensions.

topics: journal bearings, system identification, linear and non-linear systems

1. Introduction

The context of the study is a maritime industry with a fleet of *liquefied natural gas* (LNG) carriers propelled by ABB diesel-electric propulsion system (Fig. 1). An LNG carrier is a tank ship designed for transporting liquefied natural gas.

LNG carriers are highly sophisticated in terms of technology and are specially designed to transport LNG at a low temperature of −162°C. They are regarded as the "super freezer cars of the sea" and "the pearl on the crown" in the world shipbuilding industry [1]. With the diesel–electric concept design, main reciprocating engines are typically 4 stroke, dual-fuel engines that are capable of running on both liquid diesel oil and gaseous boil-off gas. As a result, the propeller of the diesel–electric propulsion is operated by an electric motor, which draws power from a diesel generator. A schematic overview of the diesel–electric system is shown in Fig. 2. Main electricity producers onboard LNG vessels are *medium voltage* (MV) electric generators driven by a prime mover, e.g., 4 stroke diesel engines. Generators convert mechanical energy derived from diesel engines into electrical energy generated as *alternating current* (AC) sinusoidal output waveform. The distribution of electrical AC power is governed and protected by MV switchboard. One of the main consumers of electricity is electric propulsion motors (Fig. 3). *Propulsion motor* (PM) is driven by MV frequency converter that modulates the frequency and torque of the electrical supply and thus controls the rotational speed (rpm — revolutions per minute, here denoted also as RPM) of the motor.

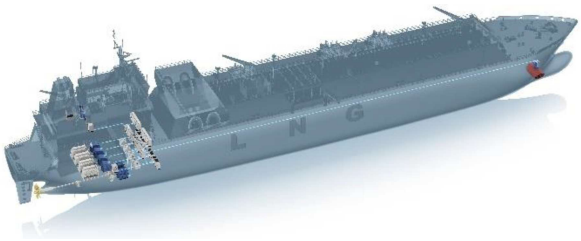

Fig. 1. LNG carrier equipped with ABB diesel electric propulsion system (manufacturer — ABB).

The mechanical power of the propulsion motor is transferred via a step-down gearbox to the main shaft ended up with a fixed-pitch propeller.

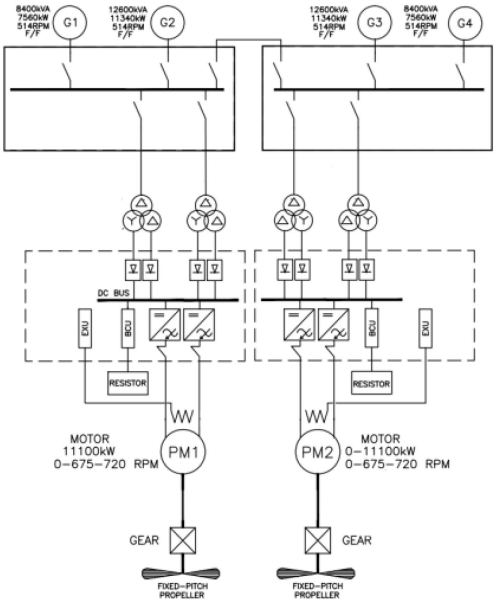

Fig. 2. Fragment of electric single line diagram (SLD) for diesel electric propulsion system (manufacturer — ABB).

Fig. 3. Electric propulsion motor (manufacturer — ABB).

Electric propulsion motors are of excited, synchronous type. They are equipped with sleeve (or plain, or journal) bearings. There are two bearings on each motor (drive and non-drive end) and two propulsion motors per vessel.

2. Journal bearings

2.1. Design

The main propulsion motor onboard LNG carrier is a critical component. Unexpected failure or stoppage of the motor forces the vessel to decrease sailing speed. That in consequence may lead to missing the time window selected for this particular LNG carrier to reach LNG terminal and to load/discharge the main cargo. Economical losses caused by such a scenario are substantial and counting in approximately 100000 USD per day of charter rate plus penalties related to delayed delivery.

Fig. 4. Sleeve bearing (manufacturer — RENK).

There are few possible failure modes that may occur in MV electric propulsion motor but for the simplicity, we categorize them by origin into two categories, namely electrical and mechanical. An example of the failure mode originated from electrical source is the one described in work [2] where the motor winding overheating occurs. Article [2] discusses methods and algorithms that are supposed to forecasted such faults. Good case of the failure mode originated from mechanical source is a subject of this article, i.e., motor bearing. We focus on journal (or sleeve or plain) type of the bearing that is used most commonly in electric propulsion motor onboard LNG carriers propelled by ABB diesel electric propulsion system.

Journal (or sleeve or plain) bearings shown in Fig 4. facilitate rotational movement between two parts.

Unlike the rolling action of a ball bearing or roller bearing, the sleeve bearing has a sliding action. When needed they can be used with lubricates or self-lubricating components to ensure smooth continuous operation.

Because they are relatively low cost and maintenance-free, sleeve bearings are used in many applications, commonly in low-speed machines such as MV propulsion motor of LNG carrier that has typically maximum rotational speed below 1000 rpm.

2.2. Condition monitoring of journal bearings

There are several factors that can damage a journal-bearing surface. Abrasive wear is one of the most common. Wear can be caused by a hard particle rubbing between the lubricated surfaces or by asperity on one surface cutting the other surface.

Wear can also result from insufficient volume of lubricant (starvation leading to boundary conditions), overheated lubricant (viscosity at operating temperature cannot support the load causing frictional heat and additional oil thinning), rough surfaces (asperities on the journal cause rubbing), imbalance (improper loading of the support element causing shock loading), journal eccentricity (egg-shaped journal causing rubbing on the high spots), and metal fatigue from improper metallurgy. Journal bearing wear can be effectively monitored by following techniques:

(i) Oil analysis to detect contamination of oil (water, dirt) that may be a cause of the wear and ferrographic analysis to monitor actual content of metal particles that are an effect of the wear and metal to metal contact of sliding elements.

(ii) Orbit plots — technique that visualizes the movement of the shaft within the bearing. It uses proximity (displacement) probes that measure actual movement between the bearing casing and the shaft. Orbit plots analysis can detect faults such as imbalance, misalignment, heavy pre-load, oil whirl and oil whip.

(iii) Vibration analysis — accelerometer mounted on the case of the bearing will provide a useable to some extent signal that helps to detect problems such as oil whirl, oil whip, and shaft rubs. However, due to the dampening effect of the fluid film, the vibration will be attenuated and the low-frequency response is limited.

To summarize techniques (i) and (ii) are the most effective but their disadvantage is the high cost of implementation. Unless the machine is equipped with proximity probes and an online oil analysis sensor during its manufacturing process, it is very costly and technically challenging to install those sensors on running system. Method (iii) is less costly and relatively easy to implement, yet does not provide a full overview about different symptoms of faulty condition. Therefore, in case techniques (i) and (ii) cannot be used, it is justified to combine method (iii) with other techniques, basing on the availability of other measurements from the motor related to its performance.

The essence of this article is to explore the possibilities of using a model-based approach for analyzing journal bearing frame temperature in order to detect anomalies related to the condition of the bearing. A similar approach has been used in work [12]. There are very few works about condition monitoring methods for journal bearing based on temperature measurements only. However, by monitoring the bearing temperature, it is expected to detect overheating of lubricant. In such a condition, viscosity of lubricant decreases, leading to oil thinning or even rubbing. Ning Ding at al. [13] involve bearing temperature measurements within

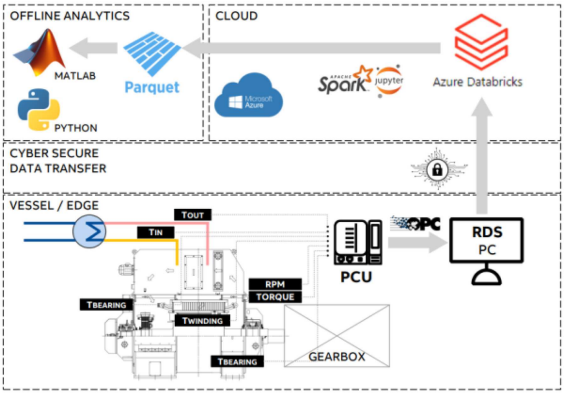

Fig. 5. Data acquisition flow diagram.

multi-sensor data set analysis that aims at generalization of learning methods. An approach with a direct model of thermo-elastic hydrodynamic lubrication (THL) is used in work [14] to find the correlation between contact potential and asperity contact. Ojaghi and Yazdandoost [15] present interesting work on detecting unwanted oil-whirl state within sleeve bearings, based on spectral analysis of motor stator current measurements. Similarly, Jung and Park in work [16]. Bearing temperature is used in machine learning algorithms to predict friction torque and friction coefficients in radial, journal bearings [17]. There is an attempt of deriving a mathematical model for a temperature change of the journal bearing presented in work [18]. Finally, Ates at al. [19] develop a data-driven methodology for indirectly determining the wear condition of the bearing by leveraging collected vibration data.

3. Data set description

3.1. Data acquisition

Data acquisition process that facilitated compilation of data set used in this work is depicted in Fig. 5.

The process consists of the following stages:

(i) Onboard the vessel, both the propulsion motor and frequency converter are equipped with a number of sensors measuring different physical properties. Examples are temperature sensors installed on the stator winding or journal bearing frame or in the cooling air ducts. The overriding control is taken by *propulsion control unit* (PCU), e.g., programmable logic controller (PLC) that receives commands from the bridge together with signals from the sensors and translates it into set points for frequency converter. PCU also acts as a local digital hub for all critical signals. The role of the data historian is taken by *remote*

diagnostic system (RDS). In principle, it is a computer onboard the vessel, connected to vital digital communication buses within diesel–electric systems. RDS computer runs diagnostic software facilitating smart acquisition of essential signals. Among others, RDS acquires also relevant signals related to the performance of the propulsion motor and for that, it subscribes to the PCU controller. Communication between RDS and PCU is based on the *open platform communications* (OPC) protocol (OLE for process control) and the RDS acts as an OPC client. Approximately 100 signals from a single PCU are acquired with sampling rates varying from fraction of a second to minutes and hours.

(ii) Cyber secure data transfer from RDS system onboard to Smart Asset Management repository in the cloud. Data packaged into 10 min long, compressed chunks are tunneled via an encrypted link over the public internet.

(iii) Once data arrive on the cloud side of this ecosystem, they are automatically imported into highly efficient storage, based on Azure Databricks technology. Data are contextualized so that are agnostic regardless of the vessel design type. Querying and exporting data out of Azure Databricks is done with the use of PySpark libraries and runs effectively on the Azure cluster. Data are dumped into a number of parquet formatted files and downloaded to physical machines, where actual discovery analysis is done with the use of Matlab and Python environments.

3.2. Scope of data

In order to create a data set used in this work, recordings from approximately 40 LNG carriers have been extracted. That translates to 80 propulsion motors and 160 instances of journal bearings. The main criterion for the selection of the vessel was data completeness. In reality, historical records for data considered in the article reach back to the year 2017. However, as the data preprocessing work for this analysis proved, the actual amount of data is smaller due to the delayed deployment of ecosystems presented in Fig. 5 and data gaps caused by temporary acquisition system outage. The total sum of all periods with good quality data across all cases analyzed in this work gives the measurement time length of almost 300 years. Out of approximately 100 different signals available within a single PCU subsystem, for journal-bearing analysis, there were approximately 23 selected. Selection was based on domain, and engineering knowledge related to the relevance of the measurements to its impact on the bearing temperature. Table I presents selected signals, grouped by similar type and origin.

Signal description. TABLE I

Signal groups		
Signal names [unit]	Fs	Description
DENDTemp, NDENDTemp [°C]	1 min	temperatures of bearing frame on drive and non-drive ends
DENDVib, NDENDVib [mm/s]	30 s	overall vibration velocity RMS values on drive and non-crive ends
MPCoolAirINTemp, MPCoolAirOUTTemp [°C]	1 min	temperatures of cooling IN and cooling OUT air
MPCoolFan1-4 [1]	1 min	ON/OFF signals for cooling fans 1–4; four signals in total
ExcE1Temp [°C]	1 mmin	phase E1 excitor winding temperature
MPWindPh1-2Temp [°C]	1 m	in total 6 signals representing stator winding temperatures on all 6 phases (U1, U2/V1, V2/W1/W2)
MPPower [%]	$<$ 1 min	electrical power of propulsion motor in % of nominal
MPSpeed [%]	$<$ 1 min	rotational speed of the shaft in % of nominal
MPTorque [%]	$<$ 1 min	electical torque of propulsion motor in % of nominal
MMode [1]	1 min	manouvering mode of the vessel according to *Automatic Identification System* (AIS) schema
RudderAngle [deg]	5 s	degrees of rudder angle
SSpeed [knots]	20 s	ship's speed over ground

Fs — sampling frequency rate,
DE — drive-end, NDE — non-drive-end

Data sets were categorized by the journal-bearing types. As a result a list of bearing types with corresponding dataset identifiers is presented in Table II. Motor types and ratings are typically the same within a single building series of ships and vary slightly across various owners. In particular, for nominal values, motor power is in the range of 11–12.5 MW, the motor voltage on the level of 2900 V, current 2×1300 A or 2700 A, rotation speed between 520 and 675 rpm.

3.3. Data cleansing

Since signals are recorded with different sampling rates it is necessary to synchronize them into the same time grid.

From the analysis of the time step response of the modelled variable that is the temperature of the bearing frame, it has been verified that the time constant of dynamic response is in the order

TABLE II

List of journal bearing types with dataset identifiers.

Bearing type	Data set identifier
R-35 (DE)/R-28 (NDE)	G1, G2, G3, G4, S1, S2, S4, S5, S6, S7, S8, S9, O2, O3, O6, O9, O10, O11, O12
L-35 (DE)/L-28 (NDE)	O1, O4, O5, O7, O8, O13, O14, O15, O17, O18, O19, O20, O21, O22, O23, O24, O25, O27

of 40–70 min. Thus, it has been arbitrarily set to retime all the signals to a common grid of 3 min intervals. Filling missing points with previous value and aggregating with maximum value from the bin. Figure 6 illustrates how the above approach handles cases with missing data due to system outage or deadband settings.

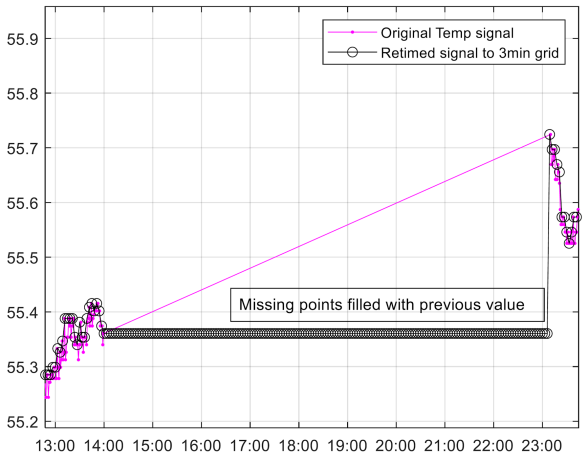

Fig. 6. Retiming effect on raw data.

4. Modelling techniques

4.1. Correlation matrix

The goal of the analysis is to model bearing *drive-end* (DE) and *non-drive end* (NDE) temperature with use of selected covariates from the dataset. Model structure, i.e., selection of covariates is done in an iterative manner with the use of the backward elimination method. This is to reduce the model size, yet achieve the best performance.

The very first step to determine the relation between covariates is to calculate the correlation matrix. As expected and shown in Fig. 7, there are strong linear correlation between bearing frame temperature and temperatures of other points of the motor. Stator windings are elements that heat up most significantly and the temperature increase is a direct effect of motor losses.

4.2. Linear models

Model selection by backward elimination is initiated with the use of continuous state-space multiple input single output (MISO) structure of the following form

$$\dot{x}(t) = A\,x(t) + B\,u(t) + K\,e(t),$$
$$y(t) = Cx(t) + Du(t) + e(t). \tag{1}$$

Here, A, B, C, D, K are state-space matrices, $u(t)$ is the input, $y(t)$ is the output, $e(t)$ is the disturbance and $x(t)$ is the vector of n states (e.g., model order).

The order of the model is selected optimally based on the Hankel matrix. For the data sets used in the calculation, the order is set typically to value 2.

For each and every model training and testing process, the training set is arbitrarily set as the initial c.a. 30% portion of the entire data set. For the model tests, the remaining part is used. Table III summarizes information about the model performances vs its structure based on selected and most representative data sets. Normalized root mean square error (NRMSE), expressed by

$$\mathrm{NRMSE} = 100 \times \left(1 - \frac{||y - \hat{y}||}{||y - \mathrm{mean}(y)||}\right), \tag{2}$$

is used as a measure of goodness of fit between the predicted model response and the actual measurement data of bearing temperatures. Interestingly, as presented on selected cases of G4-1 DE and O13-1 DE (see Table III), there are respectively two cases observed for the 2nd order linear, continuous time state-space estimation. The first case is represented by NRMSE error for G4-1 DE in Table III, where model reduction results in better performance (higher NRMSE), and the second case is for O13-1 DE, where reduction of the model structure results in worse performance (lower NRSME).

The second family of linear model used in the benchmarking was so-called ARX model. For example, autoregressive with extra input as the model input term is also included. The ARX model structure is given by

$$y(t) = a_1 y(t-1) + \ldots + a_{n_a} y(t-n_a) =$$
$$b_1 u(t-n_k) + \ldots + b_{n_b} u(t-n_b-n_k+1) + e(t), \tag{3}$$

where $y(t)$ is output at time t, n_a is the number of poles, n_b is the number of zeros, n_k is the number of dead time samples, $y(t-1), \ldots, y(t-n_a)$ — previous outputs on which current input depends, $u(t-n_k), \ldots, u(t-n_k-n_b)+1$ — previous and delayed inputs on which the current output depends.

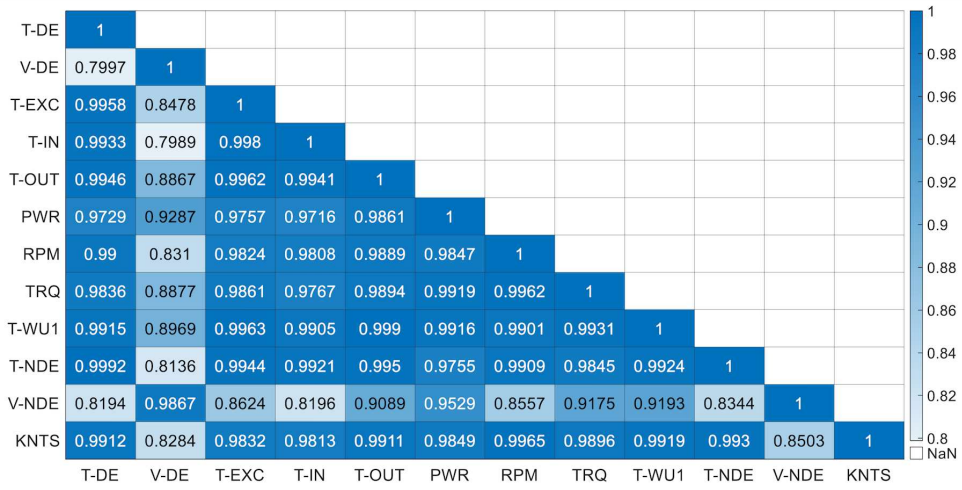

Fig. 7. Correlation matrix for selected variables.

TABLE III

Structure of linear state space models for selected datasets

ID	Model input covariates	NRMSE [%]	
		G4-1 DE	O13-1 DE
ALL	V-DE, T-IN,T-OUT, PWR, RPM, TRQ, T-WU1, T-NDE/T-DE, V-NDE	76.8	93.1
M1	RPM, PWR, V-DE, V-NDE, T-IN, T-OUT, T-NDE/T-DE	78.5	92.5
M2	RPM, PWR, T-IN, T-OUT, T-NDE/T-DE	78	92.5
M3	RPM, T-IN, T-OUT, T-NDE/T-DE	68	69
M4	RPM, T-IN, T-OUT	82.8	76.5
M5	RPM, T-IN, T-WU1	85,3	79.3
M6	RPM, T-IN, T-OUT, V-DE/V-NDE	84.1	76.3

For ARX models, only two structures have been tested that correspond to state-space model M5 and M6. As presented in Table IV, the performance of ARX models is superior to state-space model. This is due to strong, positive impact of previous outputs on which current output strongly depends.

4.3. Non-linear models

In recent years, models based on various types of *artificial neural networks* (ANN) have been increasingly used. ANNs are inherently nonlinear, so

TABLE IV

Structure of linear, ARX models for selected datasets.

ID	Model input covariates	NRMSE [%]	
		G4-1 DE	O13-1 DE
M1	RPM, T-IN, T-WU1	87.1	86
M2	RPM, T-IN, T-OUT, V-DE/V-NDE	86.6	84.8

TABLE V

Structure of non-linear models for selected datasets.

ID	Model input covariates	NRMSE [%]	
		G4-1 DE	O13-1 DE
M1	RPM, T-IN, T-WU1	90.5	89.8
M2	RPM, T-IN, T-OUT, V-DE/V-NDE	89.4	83.8

they can be used to identify processes that contain even strong nonlinearities. For time series prediction applications, models based on the classical, multilayer neural network can be used. Although such a network can reflect the dynamics of the object per se, it is possible to use external feedback. In this case, delayed values of its outputs are fed to the network input. The use of particularly popular and recently studied deep and convolutional networks in time series prediction problems seems to be too complicated at the first stage. In practice, it has been proven that a network with at least 2 hidden layers can approximate any continuous function — increasing the number of hidden layers mainly leads to an increase in computational requirements. The use of convolutional networks makes sense when we know that detecting certain features is important in the data processing process. And as such, it is mainly predisposed to classification problems.

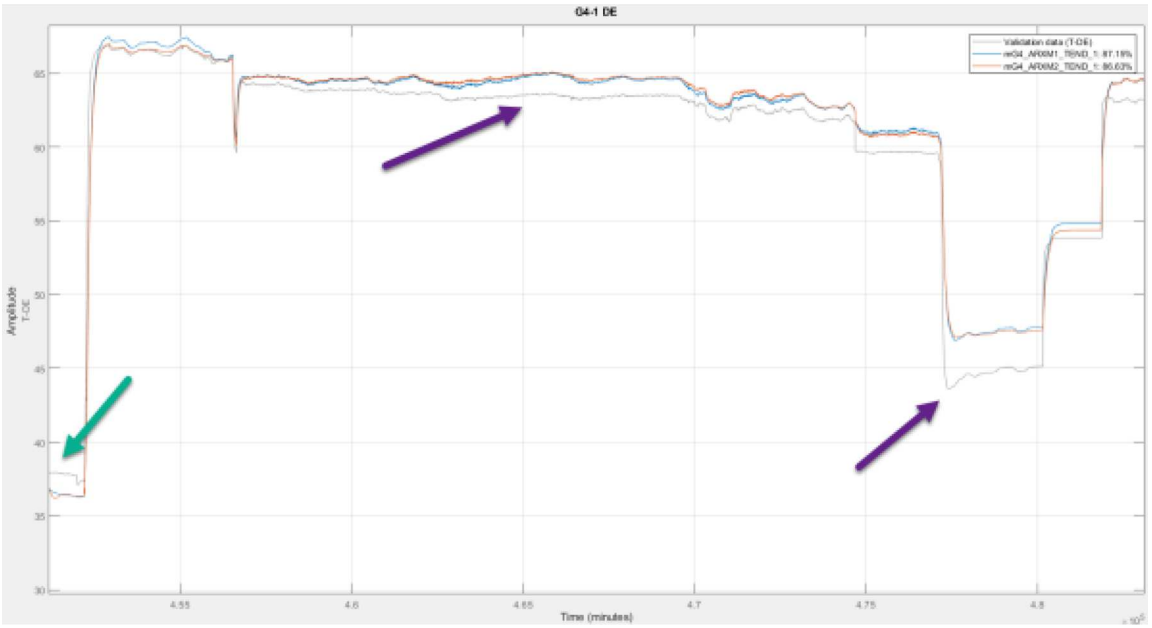

Fig. 8. Bad performance of linear models in steady-state periods.

An interesting solution seems to be the use of recurrent networks, particularly *long short-term memory* (LSTM). Such a network abandons unidirectional transmission and processing of information, assuming that individual neurons have a state — a memory of what has happened to them in the past. Generally, the main problem with recurrent networks is their complex learning process.

Due to the ability to easily estimate nonlinear phenomena and include process dynamics in the model, multilayer feedforward neural networks were selected for this paper as a starting point. A neural network with two hidden layers was trained, with the number of neurons being 2 times the number of inputs in the first hidden layer and 0.5 times the number of inputs in the second hidden layer.

The MATLAB/Simulink package was used as the basic modelling tool. The received results are in Table V.

5. Discussion

The main effort of the study presented in this work was to compile a significantly large set of field data, representing the real performance of the population of identical or very similar propulsion motors and their components. Having such a representative data set sets strong foundations for further work related to the modelling of selected physical properties of the motor to further use it in anomaly detection and actual fault identification.

The motor component of the main focus in this work is journal bearing. In order to get better understanding of signal relation, the correlation matrix has been analysed. A strong correlation with RPM is expected. The rotation speed of the shaft should have a direct impact on the lubrication oil temperature. Motor power, or torque, or a speed describe the same causality, e.g., load of the motor. They are strongly correlated with bearing temperature as well. Stator winding temperature and excitation winding temperatures are also highly correlated but in this case, it is expected, as it is related to the heat transfer between motor components. It is not obvious, however, what is the exact heat transition path between stator windings and the point of the motor where the bearing frame temperature sensor is installed. Cooling air IN and OUT temperatures may be important model covariates, provided there is a direct effect of cooling the winding into the bearing temperature. Design-wise, the excitation winding is located closer to the drive end bearing and we also see it in a higher correlation value than for non-drive end. Surprisingly, there is a low correlation between bearing temperature and bearing vibration, and further models selection proved vibration is a covariate of low significance.

Linear state-space model of order 2 shows that combination of training set versus testing set gives different results of model backward elimination selection. One may say, however, that a model based on RPM, cooling AIR IN and stator winding or excitation winding temperature gives the best results.

ARX models gave superior results over state-space and the structure excluding vibration and including stator winding temperature gave better scoring (Table IV, model M1).

In case of tested linear approximations, there has been observed quite significant bias between estimated and real values in the steady state periods.

An example is shown in Fig. 8, where purple arrows show model output bigger than actual values and green arrow shows the opposite performance.

Such an outcome indicates that the physical system has strong non-linearities most probably in the static characteristics. Linear models are not sufficient in this case and either non-linear coefficient transformation of linear models is necessary or the application of purely non-linear models is needed. The application of neural models demonstrated the validity of the assumption about the nonlinearity of the process. For both input sets to the model — M1 and M2, an improvement was observed, with greater modelling accuracy initially obtained for the M1 model with fewer inputs. This confirms the thesis about the lack of influence of vibrations on the bearing temperature.

6. Conclusions

The scope of work presented in this article allows for drawing initial conclusions about the best way of utilizing motor performance data in the diagnostics of journal bearings. It has been recognized that with the use of selected types of linear approximations, it is possible to achieve decent predictions, especially during dynamic states of the system. It has also been possible to pinpoint a model structure that performs the best and has the lowest number of covariates. There is, however, strong desire to improve predictions in the steady-state areas of the system operation. For that, including non-linear transformation of selected covariates is one way. Other way is to employ fully non-linear techniques such as neuro-fuzzy models or boosting methods could be other direction of further research. It may also be tempting to reduce the problem to building a model that only detects steady states and predicts. This is because application-wise, it is not required to find symptoms and anomalies as quickly as possible. It is more about finding them reliably. Ultimately, predictions are supposed to be used as the very first step of a more important task which is anomaly or fault detection. In this area, there is also a need to possibly step out from unsupervised data sets as was done in this work and attempt to enrich data with weakly or strongly supervised cases.

References

[1] ABB Press release, "ABB Wins Milestone Contract with China's Leading LNG Shipyard", 2015.

[2] K.H. Hellton, M. Tveten, M. Stakkeland, S. Engebretsen, O. Haug, M. Aldrin, *J. Marine Eng. Technol.* **21**, 334 (2021).

[3] N. Ding, H. Li, Q. Xin, B. Wu, D. Jiang, *Reliab. Eng. Syst. Saf.* **230**, 108966 (2023).

[4] B. Wan, J. Yang, S. Sun, *Appl. Sci.* **10**, 5199 (2020).

[5] M. Ojaghi, N. Yazdandoost, *IEEE Trans. Energy Convers.* **30**, 1537 (2015).

[6] J. Jung, Y. Park, S. Bin Lee, C. Cho, K. Kim, E. Wiedenbrug, in: *2015 IEEE Energy Conversion Congress and Exposition (ECCE)*, IEEE, 2015 p. 300.

[7] H. Bas, Y.E. Karabacak, *Tribol. Int.* **186**, 108592 (2023).

[8] R. Antunović, A. Halep, M.M. Bučko, S.R. Perić, *Therm. Sci.* **22**, 323 (2018).

[9] C. Ates, T. Höfchen, M. Witt, R. Koch, H.J. Bauer, *Sensors* **23**, 9212 (2018).